Title

Identifying Hypoperfusion in Moyamoya Disease With Arterial Spin Labeling and an [15O]-Water Positron Emission Tomography/Magnetic Resonance Imaging Normative Database

Journal

Stroke, 50(2)

ISSN

0039-2499

Authors

Fan, Audrey P
Khalighi, Mohammad M
Guo, Jia
et al.

Publication Date

2019-02-01

DOI

10.1161/strokeaha.118.023426

Peer reviewed

HHS Public Access

Author manuscript

Stroke. Author manuscript; available in PMC 2020 April 16.

Published in final edited form as:

Stroke. 2019 February ; 50(2): 373–380. doi:10.1161/STROKEAHA.118.023426.

Identifying Hypoperfusion in Moyamoya Disease With Arterial Spin Labeling and an [^{15}O]-Water Positron Emission Tomography/Magnetic Resonance Imaging Normative Database

Audrey P. Fan, PhD,
Department of Radiology Stanford University, CA

Mohammad M. Khalighi, PhD,
Stanford University, CA; Global Applied Science Lab, GE Healthcare, Menlo Park, CA

Jia Guo, PhD,
Department of Radiology, Stanford University, CA

Department of Bioengineering, University of California Riverside

Yosuke Ishii, MD,PhD,
Department of Radiology, Stanford University, CA

Department of Neurosurgery, Tokyo Medical and Dental University, Japan

Jarrett Rosenberg, PhD,
Department of Radiology Stanford University, CA

Mirwais Wardak, PhD,
Department of Radiology Stanford University, CA

Jun Hyung Park, PhD,
Department of Radiology Stanford University, CA

Bin Shen, PhD,
Department of Radiology Stanford University, CA

Dawn Holley, BS,CNMT,
Department of Radiology Stanford University, CA

Harsh Gandhi, MS,
Department of Radiology Stanford University, CA

Tom Haywood, PhD,
Department of Radiology Stanford University, CA

Correspondence to Audrey P. Fan, PhD, Lucas Center for Imaging, Stanford University, 1201 Welch Rd, Stanford CA 94305. mailto:auddie@stanford.edu.

Disclosures

Dr Khalighi is employed by General Electric Healthcare, and Dr Zaharchuk receives funding support from General Electric Healthcare. The other authors report no conflicts.

The online-only Data Supplement is available with this article at https://www.ahajournals.org/doi/suppl/10.1161/STROKEAHA.118.023426.

Prachi Singh, PhD,
Department of Radiology Stanford University, CA

Gary K. Steinberg, MD,PhD,
Department of Neurosurgery Stanford University, CA

Frederick T. Chin, PhD,
Department of Radiology Stanford University, CA

Greg Zaharchuk, MD,PhD
Department of Radiology Stanford University, CA

Abstract

Background and Purpose——Noninvasive imaging of brain perfusion has the potential to elucidate pathophysiological mechanisms underlying Moyamoya disease and enable clinical imaging of cerebral blood flow (CBF) to select revascularization therapies for patients. We used hybrid positron emission tomography (PET)/magnetic resonance imaging (MRI) technology to characterize the distribution of hypoperfusion in Moyamoya disease and its relationship to vessel stenosis severity, through comparisons with a normative perfusion database of healthy controls.

Methods——To image CBF, we acquired [^{15}O]-water PET as a reference and simultaneously acquired arterial spin labeling (ASL) MRI scans in 20 Moyamoya patients and 15 age-matched, healthy controls on a PET/MRI scanner. The ASL MRI scans included a standard single-delay ASL scan with postlabel delay of 2.0 s and a multidelay scan with 5 postlabel delays (0.7–3.0s) to estimate and account for arterial transit time in CBF quantification. The percent volume of hypoperfusion in patients (determined as the fifth percentile of CBF values in the healthy control database) was the outcome measure in a logistic regression model that included stenosis grade and location.

Results——Logistic regression showed that anterior (P<0.0001) and middle cerebral artery territory regions (P=0.003) in Moyamoya patients were susceptible to hypoperfusion, whereas posterior regions were not. Cortical regions supplied by arteries with stenosis on MR angiography showed more hypoperfusion than normal arteries (P=0.001), but the extent of hypoperfusion was not different between mild-moderate versus severe stenosis. Multidelay ASL did not perform differently from [^{15}O]-water PET in detecting perfusion abnormalities, but standard ASL overestimated the extent of hypoperfusion in patients (P=0.003).

Conclusions——This simultaneous PET/MRI study supports the use of multidelay ASL MRI in clinical evaluation of Moyamoya disease in settings where nuclear medicine imaging is not available and application of a normative perfusion database to automatically identify abnormal CBF in patients.

Keywords

cerebral blood flow; magnetic resonance imaging; Moyamoya disease; positron emission tomography

---

Moyamoya disease is characterized by progressive stenosis or occlusion of arteries at the base of the brain, which places patients at 7-fold increased risk of stroke and leads to

development of extensive collateral vessels to compensate. Although direct or combined revascularization procedures have shown efficacy in reducing the 5-year occurrence of stroke during follow-up,[1,2] the optimal surgical treatment remains unclear.[3] Few randomized trials[4,5] to evaluate these treatments have been reported to date, due in part to a lack of established biomarkers that stratify patients with high stroke risk from those who remain asymptomatic for long disease durations.[6]

Conventional angiography to visualize the lumen of the arteries has become a mainstay in Moyamoya diagnosis, but the degree of proximal stenosis may not be the only determinant of disease severity if compensation through collateral vessels is adequate. Instead, imaging of cerebral blood flow (CBF) biomarkers to characterize territory-specific perfusion[7] will likely play a large role in future clinical trials. Noninvasive perfusion imaging is technically challenging, especially if the disease pathology interacts with the imaging mechanism itself to create CBF inaccuracies, as with standard arterial spin labeling (ASL) magnetic resonance imaging (MRI) approaches.In Moyamoya populations, long arterial transit times (ATTs) through collateral pathways cause ASL hyper-intensities[8] and underestimation of CBF[9] that obscure the true perfusion status of patients and require advanced labeling strategies for accurate measurement.

The advent of simultaneous positron emission tomography (PET)/MRI technology presents a unique opportunity to quantify perfusion concurrently with ASL MRI and the [^{15}O]-water PET reference standard to inform our pathophysiological understanding of Moyamoya disease.[10] This PET/ MRI study characterized the spatial distribution of hypoperfusion in Moyamoya patients, as measured by simultaneous PET and ASL, through comparison with a normative CBF database of healthy individuals.[11] The ASL scans included a standard single-delay acquisition, as well as an advanced multidelay acquisition, that directly measures and accounts for ATTs in CBF measurement. We hypothesized that multidelay ASL more accurately identifies ischemia in patients than standard-delay ASL when compared with the PET reference and that the extent of hypoperfusion relates to the severity of vessel stenosis in Moyamoya patients.

Methods

The data that support the findings of this study are available from the corresponding author on request.

Participants

Twenty patients with Moyamoya disease undergoing evaluation for extracranial to intracranial bypass surgery in the Department of Neurosurgery at Stanford University were recruited (Table 1). All patients had a confirmed diagnosis of Moyamoya disease based on ≥1 diagnostic evaluations, including catheter cerebral angiography, MRI angiography, and computed tomography angiography. Five patients presented with unilateral disease and the rest with bilateral disease. Nine patients had a history of prior strokes, and 4 patients had undergone previous bypass surgery (mean time from surgery ranged from 6 months to 29 years). Fifteen age-matched healthy subjects with no history of neurological disorders and no contraindications to MRI were recruited. All participants provided written informed

consent for the study under approval from the Stanford University Institutional Review Board. Preliminary analysis in a subset of the patients has been reported.[10]

PET/MRI Acquisition

All images were acquired on a simultaneous time-of-flight enabled T PET/MRI scanner (SIGNA; GE Healthcare, Waukesha, WI). For PET perfusion scans, each subject received a manual, bolus injection of [^{15}O]-water (490–960 MBq) administered intravenously and PET acquisition commenced with the tracer injection. Dynamic PET frames over 4 minutes were reconstructed (30×1, 10×3, 12×5, 12×10 s) using an time-of-flight ordered subset expectation maximization algorithm with 3 iterations and 28 subsets on a 192×192 matrix. PET images were corrected for scatter, random counts, point spread function, and attenuation using a 2-point Dixon MRI scan and atlas-based attenuation correction.[12] The [^{15}O]-water PET scan was repeated (separated by 15 minutes) to assess intrasession reproducibility of CBF.

Simultaneously with each PET scan, 2 ASL MRI acquisitions were performed with pseudo-continuous labeling. Each ASL scan had a 3-dimensional fast spin echo readout with stack-of-spirals readout trajectory and similar scan time of 5 minutes. The standard ASL scan was acquired with consensus parameters,[13] including labeling duration of 1.5 s and a single postlabel delay (PLD) of 2.025 s. The multidelay ASL scan was acquired with a longer labeling duration of 2.0 s and 5 sequential PLD times, evenly spaced between 0.7 and 3.0 s. The use of multiple PLDs allowed for measurement of ATT in each voxel to correct the CBF measurements for variable ATTs.[14] The standard ASL scan had an in-plane resolution of 3.7 mm, whereas the multidelay acquisition had an in-plane resolution of 5.8 mm; through-plane resolution was 4 mm for both scans. ASL acquisitions were also repeated in each subject, simultaneously with the second PET scan, to assess scan-rescan variability.

All subjects also received 3-dimensional T_1-weighted MRI with an inversion-prepared, fast spoiled gradient recalled sequence for anatomic registration. Time-of-flight MR angiography (repetition time, 22.0 ms; echo time, 2.4 ms; in-plane resolution, 0.43 mm) was performed to visualize the cervical arteries. In patients, additional MRI angiograms were acquired at the Circle of Willis to characterize the stenosis in major cerebral arteries.

CBF Quantification

Image-derived input functions of the [^{15}O]-water tracer were extracted from dynamic PET signal in the carotid arteries, using an image-based method[15] that corrects for spill-in and spill-out artifacts with high-resolution segmentations of the cervical MRI angiograms. Parametric maps of CBF were then modeled from the input function and dynamic PET data using a 1-tissue compartment model in PMOD software (version 3.8; PMOD Technologies, Zurich, Switzerland).

Quantitative CBF maps from ASL MRI were generated by calibrating the ASL difference signal with a proton density-weighted reference image (saturation time, 2.0 s). For standard ASL, a 1-compartment model was used,[13] assuming a T_1 relaxation in arterial blood of T_{1a}=1.65 s and an average partition coefficient in the brain of 0.9. For multidelay ASL, a map of ATT was first estimated from the ASL signal evolution over the 5 acquired PLDs. A

2-compartment model,[14] which incorporates the estimated ATT and different T_1 relaxation times in blood versus tissue compartments (assuming $T_{1,tissue}$ =1.2 s), was then adopted to quantify CBF.

Database Approach

Normative perfusion databases were generated from the healthy control CBF maps, separately for PET and for each ASL sequence. All healthy CBF images were registered to the Montreal Neurological Institute 2-mm brain template in Statistical Parametric Mapping (SPM) software, with use of the individual's T_1-weighted anatomic scan as a reference. The PET and ASL healthy CBF databases were compared with voxel-wise parametric testing in SPM12 (http://www.fil.ion.ucl.ac.uk/spm/software/spm12), using a significance level of P=0.01 after adjusting to control for false discovery rate at the 0.05 level. Scan-rescan reproducibility of the databases was assessed with coefficient of variation (CoV; SD of the difference between the 2 scans, divided by the mean of the 2 scans across subjects).

To identify pathophysiology, perfusion images from the Moyamoya patients were also registered to the Montreal Neurological Institute template and compared with the healthy database. All perfusion maps were normalized to the cerebellum individually to account for global differences in CBF between individuals. Each patient's PET scan was then compared with the PET healthy database, and each ASL scan was compared with the corresponding ASL database. Voxels with hypoperfusion (defined as less than fifth percentile of CBF in healthy controls) were identified from this comparison and displayed on an inflated cortical surface using SUMA surface mapping software.[16]

Stenosis Severity and Statistical Regression Analysis

In Moyamoya patients, the severity of stenosis of the anterior, middle, and posterior cerebral arteries were graded as normal, mild-moderate, or severe in consensus by 2 experienced neuroradiologists (Drs Zaharchuk and Ishii). This grading scale considers stenosis of the supraclinoid internal carotid artery as both anterior cerebral artery (ACA) and middle cerebral artery (MCA) disease.[17] Perfusion was assessed in 6 perfusion territories corresponding to each cerebral artery (anterior, middle, posterior; left, and right) based on 2 slice locations of the Alberta Stroke Programme Early Computed Tomography Score system.

Multivariable fractional logistic regression was performed in patients to model the relationship between hypoperfusion and the region location, stenosis severity, and image modality.[18] The primary outcome measure was the proportion of voxels in each region with hypoperfusion. The independent factors included into the regression were region location (anterior, middle, posterior); stenosis grade (normal, mild-moderate, severe); and image modality (PET, standard ASL, multidelay ASL). Each patient contributed 6 CBF observations (corresponding to perfusion territories) per image modality to the regression, for a total of 18 CBF values. The regression model corrected for multiple comparisons and adjusted for clustering within patients, with a P significance level of 0.05. Additional statistics to evaluate coefficients of variation and perfusion thresholds were computed using paired t tests (when comparing healthy to patient groups) or 1-way ANOVA followed by

Tukey-Kramer post hoc tests (when comparing between regions or image modalities). Statistical analyses were done using Stata 15.1 (StataCorp LP, College Station, TX).

Results

Patient Stenosis Ratings

Across the Moyamoya patients, 40.0% of cerebral arteries were normal, 32.5% had mild-moderate stenosis, and 27.5% were severely stenosed or occluded (Table 1). Unlike the ACAs and MCAs, there were no PCAs with severe stenosis ($P<0.001$ by Fisher exact test). Severe stenosis was also more common in the MCAs than in the ACAs, although the difference was marginal ($P=0.045$).

Normative Perfusion Databases and Percentile Thresholds

Normative CBF databases from the healthy volunteers exhibited similar global perfusion values and were largely concordant between ASL and PET in cortical tissues, which is the focus of the perfusion assessment in Moyamoya patients (Figure 1). However, parametric statistical mapping revealed that standard ASL overestimated CBF in white matter and deep cortical tissues and underestimated CBF in the basal ganglia compared with the PET reference. Fewer voxels with systematic bias were observed between multidelay ASL and PET, especially in the white matter (which has longer ATTs) and deep gray matter.

ASL scans had low scan-rescan CoV of CBF across the cortex (7.1% and 7.7% for standard and multidelay ASL, respectively), and better reproducibility than PET scans (11.5%), $P<10^{-10}$ (Figure I in the online-only Data Supplement). The intersubject CoV was considerably higher in patients than in healthy volunteers ($P<10^{-10}$), which is expected because the intersubject CoV reflects variable pathophysiology across Moyamoya patients (Figure II in the online-only Data Supplement). In Moyamoya cases, the intersubject CoV was significantly higher than the scan-rescan CoV for each image modality ($P<10^{-10}$). This suggests that a direct comparison of patient CBF to the healthy perfusion database has sufficient sensitivity to detect abnormal perfusion.

Across all cortical regions, the threshold for hypoperfusion from the normative database was similar for [^{15}O]-water PET (29.5±3 mL/100 g per minute), multidelay ASL (28.4±3 mL/100 g per minute), and standard ASL (28.4±2 mL/100 g per minute; Table I in the online-only Data Supplement). Perfusion thresholds for regions corresponding to the MCA were slightly higher than for regions supplied by the ACA ($P=0.002$).

Regional Distribution of Abnormal Perfusion in Moyamoya Patients

Figure 2 shows a female patient with bilateral Moyamoya disease, with prior cortical infarcts on the raw perfusion images that are readily identified as hypoperfused areas on [^{15}O]-water PET. More subtle areas of hypoperfusion in the right hemisphere, corresponding to known stenosis of the right ACA, were also identified. Although the areas of hypoperfusion were visually similar between PET and multidelay ASL images, standard ASL exaggerated the extent of hypoperfusion in this patient.

Across the entire Moyamoya group, [^{15}O]-water PET identified that cortical regions supplied by the ACAs and MCAs in both hemispheres were prone to hypoperfusion when compared with the healthy group (Figure 3). This perfusion pattern was recapitulated by multidelay ASL, but standard ASL overestimated the visual extent and frequency with which patients showed hypoperfusion compared with the PET scans. Low CBF was not observed in the PCA territory, consistent with the fact that most of the PCAs (75%) in the patients were rated as normal.

Regression Model

Logistic regression identified several significant, independent predictors of hypoperfusion in Moyamoya patients (Table 2). Anterior cortical regions showed the most voxels with hypoperfusion, significantly more than middle (odds ratio, 1.56; P=0.037) and posterior regions (odds ratio, 3.85; P<0.001; Figure 4). The MCA territory also exhibited more hypoperfusion than PCA territories (P=0.003). Compared with normal regions, areas supplied by arteries with mild-moderate stenosis (odds ratio=2.80, P<0.001) and severe stenosis (odds ratio, 3.08; P=0.001) had greater number of hypoperfused voxels. However, hypoperfusion was not different between mild-moderate versus severe artery stenosis (P=0.77). Standard ASL detected more voxels with hypoperfusion than PET (P=0.003) and multidelay ASL (P=0.013). The number of low-CBF voxels, however, did not differ between multidelay ASL and PET (P=0.45).

Discussion

This study supports the use of noninvasive, multidelay ASL MRI in clinical evaluation of Moyamoya disease and a normative perfusion database to identify altered CBF in patients. CBF thresholds for hypoperfusion were determined for each ASL MRI sequence and the [^{15}O]-water PET reference in healthy volunteers, and successfully identified abnormal perfusion in Moyamoya patients, consistent with their disease location and the severity of vessel stenosis.

Compared with age-matched controls, Moyamoya patients exhibited low CBF in anterior and middle cortical regions that were consistent with stenosis of the internal carotid artery and proximal ACAs and MCAs. These vascular territories are known to be commonly affected, whereas the posterior circulation is relatively preserved, based on histopathologic studies of Moyamoya disease[19] and previous CBF imaging with xenon computed tomography.[7] Accurate identification of hypoperfusion is of critical importance as a quantitative, objective biomarker to evaluate the efficacy of new revascularization therapies.[20] In a longitudinal SPECT study of 60 Moyamoya patients who underwent superficial temporal artery-MCA bypass surgery, reduced CBF in the MCA territory improved by 9.1 mL/100 g per minute at 6 months postsurgery.[2] The current study demonstrated that noninvasive MRI, in particular, multidelay ASL, identifies visually and statistically similar hypoperfused areas in Moyamoya patients as the [^{15}O]-water PET reference. CBF thresholds for hypoperfusion were also similar between PET and multidelay ASL, with MCA territories having higher threshold values than other territories, likely because they receive a majority (21%) of total blood inflow to the brain.[21] Furthermore, multidelay ASL

had a reproducibility of 7.7% (3.5 mL/100g per minute) in Moyamoya patients, suitable for monitoring expected postsurgical changes in CBF and outperforming PET (11.5%, 7 mL/100 g per minute) in reliability.

In the regression model, baseline hypoperfusion was significantly greater in areas supplied by pathological arteries (mild-moderate or severe) compared with normal arteries in Moyamoya patients. This observation agrees with prior ASL reports in Moyamoya disease that CBF decreases with severity of the intracranial arterial steno-occlusions as scored on conventional angiography.[22] However, CBF in this study did not differ between territories supplied by arteries of mild-moderate versus severe stenosis grades. This may reflect the fact that baseline perfusion is not determined solely by the severity of anatomic vessel lesions, but depends on individual clinical status, integrity of previous bypass surgery, and collateral patterns.[23] Direct measurement of CBF and cerebrovascular reactivity in response to a vasodilation challenge is expected to more closely reflect the brain's current hemodynamic state than traditional angiographic rating.[17,24] In particular, impaired cerebrovascular reactivity and the presence of vascular steal on challenge tests have been linked to poor collateralization in Moyamoya disease and impaired tissue autoregulation to receive sufficient oxygen.[25]

Methodologically, this study provides evidence that standard ASL acquisition parameters[13] are not suitable for evaluation of cerebrovascular conditions with prolonged ATT. Standard ASL dramatically overestimated the extent of hypoperfusion in our Moyamoya patients relative to the PET reference because the labeled blood had not yet arrived at the imaging slice at the time of acquisition (a single relatively short PLD). This finding is consistent with previous comparison studies between single-delay ASL and PET in similar patient cohorts.[26] Although the CBF thresholds may be adjusted, the measurement noise of standard ASL may limit its identification accuracy even with a different hypoperfusion threshold. Alternatively, multidelay ASL with kinetic modeling more strongly correlates with PET perfusion even in severe cerebrovascular disease, because it corrects for ATT effects.[27] In this study, the areas of hypoperfusion detected by multidelay ASL in patients were not different from PET and thus accurate. This corroborates previous recommendations to assess perfusion in Moyamoya disease using multidelay ASL acquisition with an extended PLD range.[10]

The novel use of simultaneous PET/MRI here to create a normative CBF database allowed imaging of the same brain perfusion state by both modalities. This removed the need to control for CBF variability that occurs between scan sessions because of caffeine consumption and diurnal variations and enabled a fair comparison between the acquisitions.[28] Using [^{15}O]-water PET as an established reference, however, the healthy ASL databases in this study exhibited regional limitations. For instance, CBF in deep gray nuclei is underestimated by standard ASL and to a lesser extent by multidelay ASL, which is consistent with previous voxel-wise comparisons.[29] As a result, accurate perfusion assessment with ASL in the basal ganglia, which is of significant interest in movement disorders, such as Parkinson disease, may be difficult. In addition, although the regional distribution of [^{15}O]-water is robust to long ATTs, the image-derived input functions have

not been extensively validated and may have different CBF thresholds compared to PET with arterial blood sampling.

In its current form, the PET/MRI perfusion database is limited by a small sample size that may not be broadly generalizable. Moyamoya disease typically has an early clinical presentation, and the healthy control and patient groups were age-matched in this study (mean age of 36.8 and 40.9 years, respectively). However, CBF is expected to decline with age, with as much as 37% reduction from age ranges of 19 to 29 years to 80 to 89 years[30] from MRI and PET imaging studies. Furthermore, as aging is observed to increase ATT,[31] various ASL methods have differential sensitivity to these physiological changes. Therefore, it will be valuable to build a PET/MRI database of CBF stratified by age decade with added studies in elderly controls. Similar considerations also apply for sex, as females may benefit from a neuroprotective effect of progesterone and estrogen, and require higher CBF thresholds to identify hypoperfusion. Nonetheless, this work demonstrates the value of a healthy database to detect perfusion abnormalities and is suitable for other physiological biomarkers, such as cerebrovascular reactivity.

Complementary to CBF, additional hemodynamic imaging studies are needed to clarify the compensatory mechanisms in Moyamoya disease. Because patients experience highly variable compensation for similar stenosis of large vessels, imaging of collaterals and oxygenation at the tissue level is critical and has implications for predicting operative complications and risk of hemorrhage. The presence of collaterals prolongs the mean transit times of arterial blood[32] and create hyper-intensities on ASL images that result from slow flow in collateral vessels[8] and inappropriate application of tracer kinetic models, particularly in the posterior circulation (Figure III in the online-only Data Supplement). Extensive basal collateralization has also been linked to increased tissue oxygen extraction fraction and lower cerebral metabolic rate of oxygen by [^{15}O]-oxygen gas PET in the MCA territory of Moyamoya patients.[33,34] Future work correlating the presence of collaterals (with ATT), cerebro vascular reactivity, and oxygen metabolism will elucidate pathophysiological mechanisms in Moyamoya disease and can take advantage of MRI-based $CMRO_2$ and oxygen extraction fraction scans[24,35] that are more accessible than [^{15}O]-PET in patients.

Conclusions

In this study, noninvasive simultaneous PET/MRI was used to create a normative perfusion database and identify abnormal CBF in Moyamoya patients through quantitative comparison in an automated, objective manner. Location (anterior, middle) of cortical tissue and stenosis severity of the feeding cerebral artery were identified as critical, independent predictors of hypoperfusion in Moyamoya patients. Our multimodal approach demonstrated agreement between multidelay ASL and PET for assessment of hypoperfusion, thus supporting the use of ASL MRI for accurate CBF assessment of Moyamoya patients in settings where nuclear medicine imaging is not available.

Supplementary Material

Refer to Web version on PubMed Central for supplementary material.

Acknowledgments

We thank Praveen Gulaka for instrumental support in the imaging studies. We also thank Andrea Otte, Deseray Altamirano, and Teresa Bell-Stephens for tremendous efforts in patient recruitment.

Sources of Funding

This study was funded by General Electric Healthcare, National Institutes of Health grant 1K99NS102884, and the Stanford Neurosciences Institute Interdisciplinary Scholar Award.

References

1. Kim T, Oh CW, Kwon OK, Hwang G, Kim JE, Kang HS, et al. Stroke prevention by direct revascularization for patients with adult-onset moyamoya disease presenting with ischemia. J Neurosurg. 2016;124:1788–1793. doi: 10.3171/2015.6.JNS151105 [PubMed: 26636391]
2. Cho WS, Kim JE, Kim CH, Ban SP, Kang HS, Son YJ, et al. Long-term outcomes after combined revascularization surgery in adult moyamoya disease. Stroke. 2014;45:3025–3031. doi: 10.1161/STR0KEAHA.114.005624 [PubMed: 25184359]
3. Macyszyn L, Attiah M, Ma TS, Ali Z, Faught R, Hossain A, et al. Direct versus indirect revascularization procedures for moyamoya disease: a comparative effectiveness study. J Neurosurg. 2017;126:1523–1529. doi: 10.3171/2015.8.JNS15504 [PubMed: 27471892]
4. Miyamoto S, Yoshimoto T, Hashimoto N, Okada Y, Tsuji I, Tominaga T, et al.; JAM Trial Investigators. Effects of extracranial-intracranial bypass for patients with hemorrhagic moyamoya disease: results of the Japan Adult Moyamoya Trial. Stroke. 2014;45:1415–1421. doi: 10.1161/STR0KEAHA.113.004386 [PubMed: 24668203]
5. Takahashi JC, Funaki T, Houkin K, Inoue T, Ogasawara K, Nakagawara J, et al.; JAM Trial Investigators. Significance of the hemorrhagic site for recurrent bleeding: prespecified analysis in the Japan Adult Moyamoya Trial. Stroke. 2016;47:37–43. doi: 10.1161/STR0KEAHA.115.010819 [PubMed: 26645256]
6. Cho WS, Chung YS, Kim JE, Jeon JP, Son YJ, Bang JS, et al. The natural clinical course of hemodynamically stable adult moyamoya disease. J Neurosurg. 2015;122:82–89. doi: 10.3171/2014.9.JNS132281 [PubMed: 25361479]
7. Schubert GA, Czabanka M, Seiz M, Horn P, Vajkoczy P, Thome C. Perfusion characteristics of Moyamoya disease: an anatomically and clinically oriented analysis and comparison. Stroke. 2014;45:101–106. doi: 10.1161/STR0KEAHA.113.003370 [PubMed: 24193795]
8. Zaharchuk G, Do HM, Marks MP, Rosenberg J, Moseley ME, Steinberg GK. Arterial spin-labeling MRI can identify the presence and intensity of collateral perfusion in patients with moyamoya disease. Stroke. 2011;42:2485–2491. doi: 10.1161/STR0KEAHA.111.616466 [PubMed: 21799169]
9. Yoneda K, Harada M, Morita N, Nishitani H, Uno M, Matsuda T. Comparison of FAIR technique with different inversion times and post contrast dynamic perfusion MRI in chronic occlusive cerebrovascular disease. Magn Reson Imaging. 2003;21:701–705. [PubMed: 14559333]
10. Fan AP, Guo J, Khalighi MM, Gulaka PK, Shen B, Park JH, et al. Long-delay arterial spin labeling provides more accurate cerebral blood flow measurements in Moyamoya patients: a simultaneous positron emission tomography/MRI study. Stroke. 2017;48:2441–2449. doi: 10.1161/STR0KEAHA.117.017773 [PubMed: 28765286]
11. Blauwblomme T, Lemaitre H, Naggara O, Calmon R, Kossorotoff M, Bourgeois M, et al. Cerebral blood flow improvement after indirect revascularization for pediatric Moyamoya disease: a statistical analysis of arterial spin-labeling MRI. AJNR Am J Neuroradiol. 2016;37:706–712. doi: 10.3174/ajnr.A4592 [PubMed: 26585258]
12. Sekine T, Buck A, Delso G, Ter Voert EE, Huellner M, Veit-Haibach P, et al. Evaluation of atlas-based attenuation correction for integrated PET/ MR in human brain: application of a head atlas and comparison to true CT-based attenuation correction. J Nucl Med. 2016;57:215–220. doi: 10.2967/jnumed.115.159228 [PubMed: 26493207]
13. Alsop DC, Detre JA, Golay X, Günther M, Hendrikse J, Hernandez-Garcia L, et al. Recommended implementation of arterial spin-labeled perfusion MRI for clinical applications: a consensus of the

ISMRM perfusion study group and the European consortium for ASL in dementia. Magn Reson Med. 2015;73:102–116. doi: 10.1002/mrm.25197 [PubMed: 24715426]

14. Dai W, Robson PM, Shankaranarayanan A, Alsop DC. Reduced resolution transit delay prescan for quantitative continuous arterial spin labeling perfusion imaging. Magn Reson Med. 2012;67:1252–1265. doi: 10.1002/mrm.23103 [PubMed: 22084006]
15. Khalighi MM, Deller TW, Fan AP, Gulaka PK, Shen B, Singh P, et al. Image-derived input function estimation on a T0F-enabled PET/MR for cerebral blood flow mapping. J Cereb Blood Flow Metab. 2018;38:126–135. doi: 10.1177/0271678X17691784 [PubMed: 28155582]
16. Saad ZS, Reynolds RC. SUMA. Neuroimage. 2012;62:768–773. doi: 10.1016/j.neuroimage.2011.09.016 [PubMed: 21945692]
17. Federau C, Christensen S, Zun Z, Park SW, Ni W, Moseley M, et al. Cerebral blood flow, transit time, and apparent diffusion coefficient in moyamoya disease before and after acetazolamide. Neuroradiology. 2017;59:5–12. doi: 10.1007/s00234-016-1766-y [PubMed: 27913820]
18. Papke LE, Wooldridge JM. Econometric methods for fractional response variables with an application to 401(k) plan participation rates. J Appl Econom. 1996;11:619–632.
19. Fukui M, Kono S, Sueishi K, Ikezaki K. Moyamoya disease. Neuropathology. 2000;20(suppl):S61–S64. [PubMed: 11037190]
20. Kazumata K, Tha KK, Uchino H, Shiga T, Shichinohe H, Ito M, et al. Topographic changes in cerebral blood flow and reduced white matter integrity in the first 2 weeks following revascularization surgery in adult moyamoya disease. J Neurosurg. 2017;127:260–269. doi: 10.3171/2016.6.JNS16653 [PubMed: 27588593]
21. Zarrinkoob L, Ambarki K, Wàhlin A, Birgander R, Eklund A, Malm J. Blood flow distribution in cerebral arteries. J Cereb Blood Flow Metab. 2015;35:648–654. doi: 10.1038/jcbfm.2014.241 [PubMed: 25564234]
22. Noguchi T, Kawashima M, Nishihara M, Hirai T, Matsushima T, Irie H. Arterial spin-labeling MR imaging in Moyamoya disease compared with clinical assessments and other MR imaging findings. Eur J Radiol. 2013;82:e840–e847. doi: 10.1016/j.ejrad.2013.08.040 [PubMed: 24055185]
23. Nariai T, Matsushima Y, Imae S, Tanaka Y, Ishii K, Senda M, et al. Severe haemodynamic stress in selected subtypes of patients with moyamoya disease: a positron emission tomography study. J Neurol Neurosurg Psychiatry. 2005;76:663–669. doi: 10.1136/jnnp.2003.025049 [PubMed: 15834024]
24. Ni WW, Christen T, Rosenberg J, Zun Z, Moseley ME, Zaharchuk G. Imaging of cerebrovascular reserve and oxygenation in Moyamoya disease. J Cereb Blood Flow Metab. 2017;37:1213–1222. doi: 10.1177/0271678X16651088 [PubMed: 27207169]
25. Heyn C, Poublanc J, Crawley A, Mandell D, Han JS, Tymianski M, et al. Quantification of cerebrovascular reactivity by blood oxygen level-dependent MR imaging and correlation with conventional angiography in patients with Moyamoya disease. AJNR Am J Neuroradiol. 2010;31:862–867. doi: 10.3174/ajnr.A1922 [PubMed: 20075092]
26. Goetti R, Warnock G, Kuhn FP, Guggenberger R, O'Gorman R, Buck A, et al. Quantitative cerebral perfusion imaging in children and young adults with Moyamoya disease: comparison of arterial spin-labeling- MRI and H(2)[(15)O]-PET. AJNR Am J Neuroradiol. 2014;35:1022–1028. doi: 10.3174/ajnr.A3799 [PubMed: 24335546]
27. Hara S, Tanaka Y, Ueda Y, Hayashi S, Inaji M, Ishiwata K, et al. Noninvasive evaluation of CBF and perfusion delay of Moyamoya disease using arterial spin-labeling MRI with multiple postlabeling delays: comparison with 15O-Gas PET and DSC-MRI. AJNR Am J Neuroradiol. 2017;38:696–702. doi: 10.3174/ajnr.A5068 [PubMed: 28209582]
28. Fan AP, Jahanian H, Holdsworth SJ, Zaharchuk G. Comparison of cerebral blood flow measurement with [15O]-water positron emission tomography and arterial spin labeling magnetic resonance imaging: a systematic review. J Cereb Blood Flow Metab. 2016;36:842–861. doi: 10.1177/0271678X16636393 [PubMed: 26945019]
29. Heijtel DF, Mutsaerts HJ, Bakker E, Schober P, Stevens MF, Petersen ET, et al. Accuracy and precision of pseudo-continuous arterial spin labeling perfusion during baseline and hypercapnia: a head-to-head comparison with 15O H2O positron emission tomography. Neuroimage. 2014;92:182–192. doi: 10.1016/j.neuroimage.2014.02.011 [PubMed: 24531046]

30. Buijs PC, Krabbe-Hartkamp MJ, Bakker CJ, de Lange EE, Ramos LM, Breteler MM, et al. Effect of age on cerebral blood flow: measurement with ungated two-dimensional phase-contrast MR angiography in 250 adults. Radiology. 1998;209:667–674. doi: 10.1148/radiology.209.3.9844657 [PubMed: 9844657]

31. Dai W, Fong T, Jones RN, Marcantonio E, Schmitt E, Inouye SK, et al. Effects of arterial transit delay on cerebral blood flow quantification using arterial spin labeling in an elderly cohort. J Magn Reson Imaging. 2017;45:472–481. doi: 10.1002/jmri.25367 [PubMed: 27384230]

32. Togao O, Mihara F, Yoshiura T, Tanaka A, Noguchi T, Kuwabara Y, et al. Cerebral hemodynamics in Moyamoya disease: correlation between perfusion-weighted MR imaging and cerebral angiography. AJNR Am J Neuroradiol. 2006;27:391–397. [PubMed: 16484417]

33. Piao R, Oku N, Kitagawa K, Imaizumi M, Matsushita K, Yoshikawa T, et al. Cerebral hemodynamics and metabolism in adult moyamoya disease: comparison of angiographic collateral circulation. Ann Nucl Med. 2004;18:115–121. [PubMed: 15195758]

34. Kuroda S, Kashiwazaki D, Hirata K, Shiga T, Houkin K, Tamaki N. Effects of surgical revascularization on cerebral oxygen metabolism in patients with Moyamoya disease: an 15O-gas positron emission tomographic study. Stroke. 2014;45:2717–2721. doi: 10.1161/STROKEAHA.114.006009 [PubMed: 25116870]

35. Watchmaker JM, Juttukonda MR, Davis LT, Scott AO, Faraco CC, Gindville MC, et al. Hemodynamic mechanisms underlying elevated oxygen extraction fraction (OEF) in moyamoya and sickle cell anemia patients. J Cereb Blood Flow Metab. 2018;38:1618–1630. doi: 10.1177/0271678X16682509 [PubMed: 28029271]

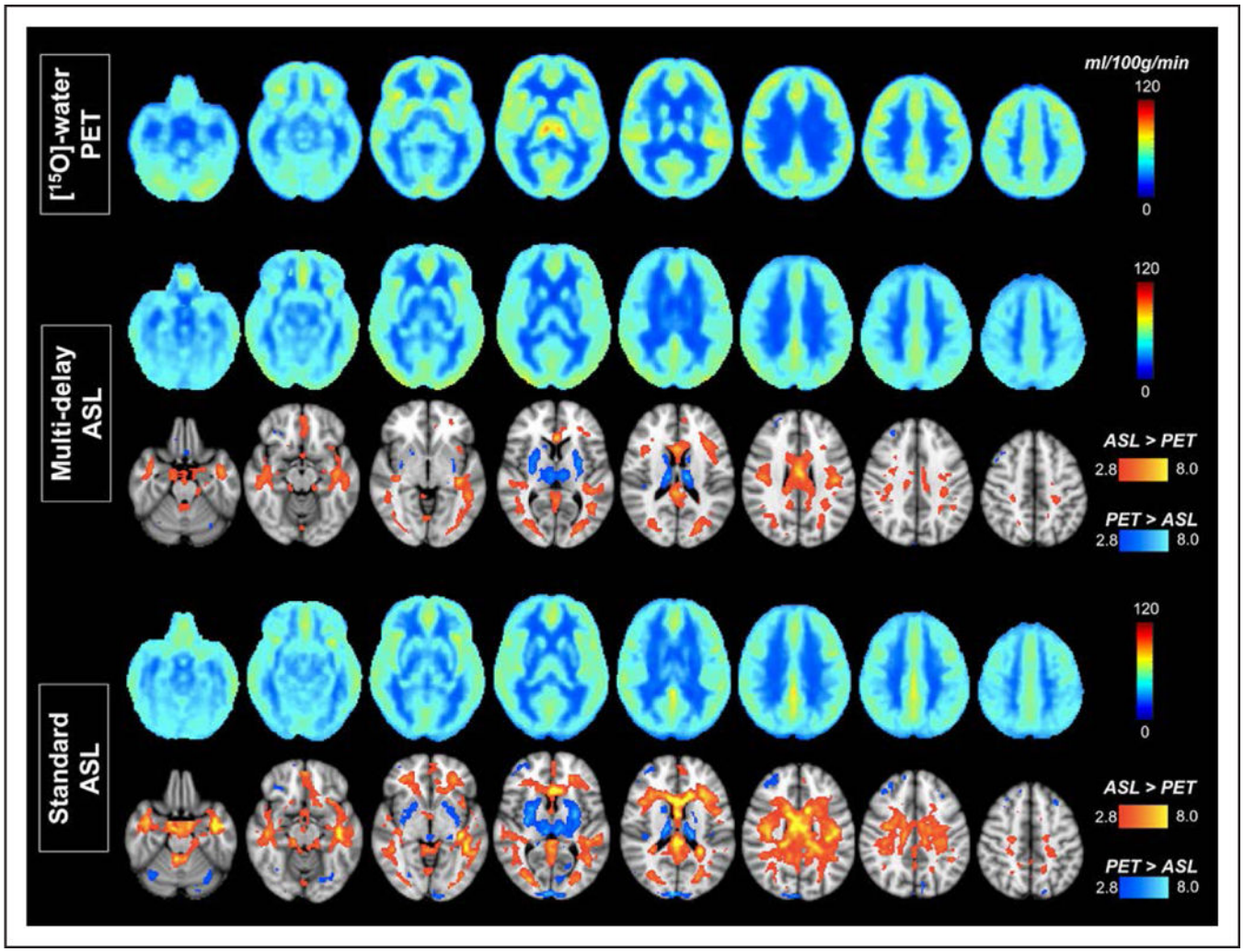

Figure 1.

Normative perfusion databases of mean cerebral blood flow (CBF) in 15 healthy volunteers (mean age 40.9 y, 8 female) measured by [^{15}O]-water positron emission tomography (PET), multidelay arterial spin labeling (ASL) and standard single-delay ASL magnetic resonance imaging. Voxel-wise parametric testing reveals areas of overestimation (red) and underestimation (blue) of CBF by each ASL method as compared to the PET reference. Significant voxels are shown at the P=0.01 level with control for false discovery rate at the P=0.05 level.

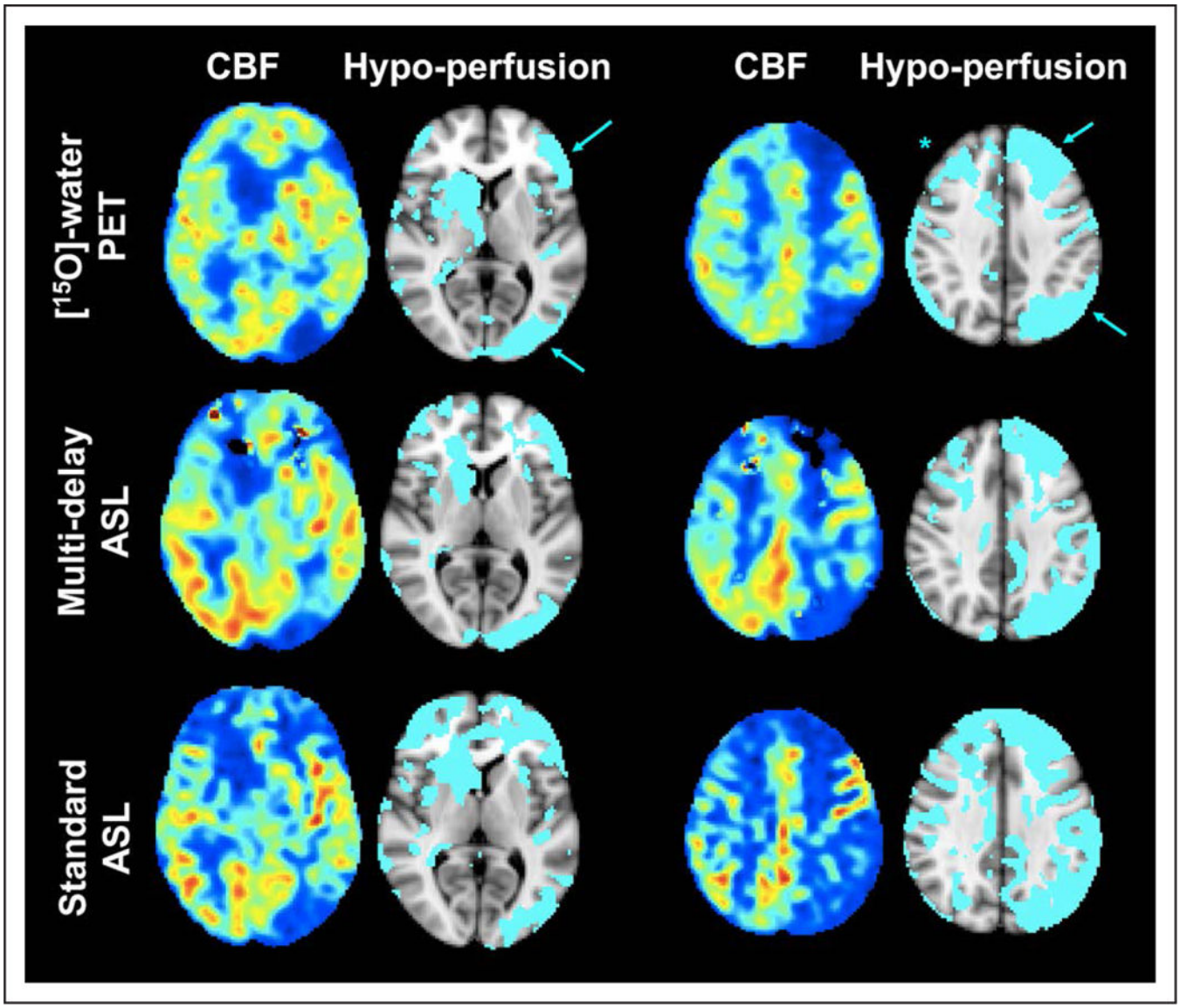

Figure 2.

Cerebral blood flow (CBF) images from a 25-y-old, female patient with bilateral Moyamoya disease. Areas of hypoperfusion are shown after comparison to the healthy CBF database for each image modality. For [^{15}O]-water positron emission tomography (PET) images, areas of hypoperfusion (arrows) are seen prominently in areas of previous infarct in the left hemisphere but also more subtly within the right anterior cerebral artery territory (asterisk). Similar areas of hypoperfusion are identified with multidelay arterial spin labeling (ASL), but the extent of hypoperfusion is overestimated on standard ASL scans.

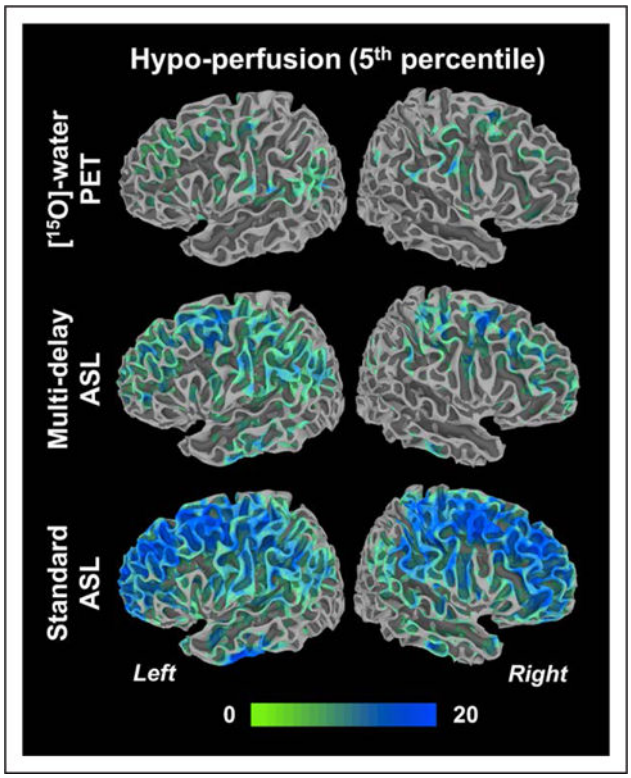

Figure 3.

Number of Moyamoya patients in the group (*N*=20) that showed hypoperfusion at each location in the inflated cortical surface compared with the healthy cerebral blood flow database. ASL indicates arterial spin labeling; and PET, positron emission tomography.

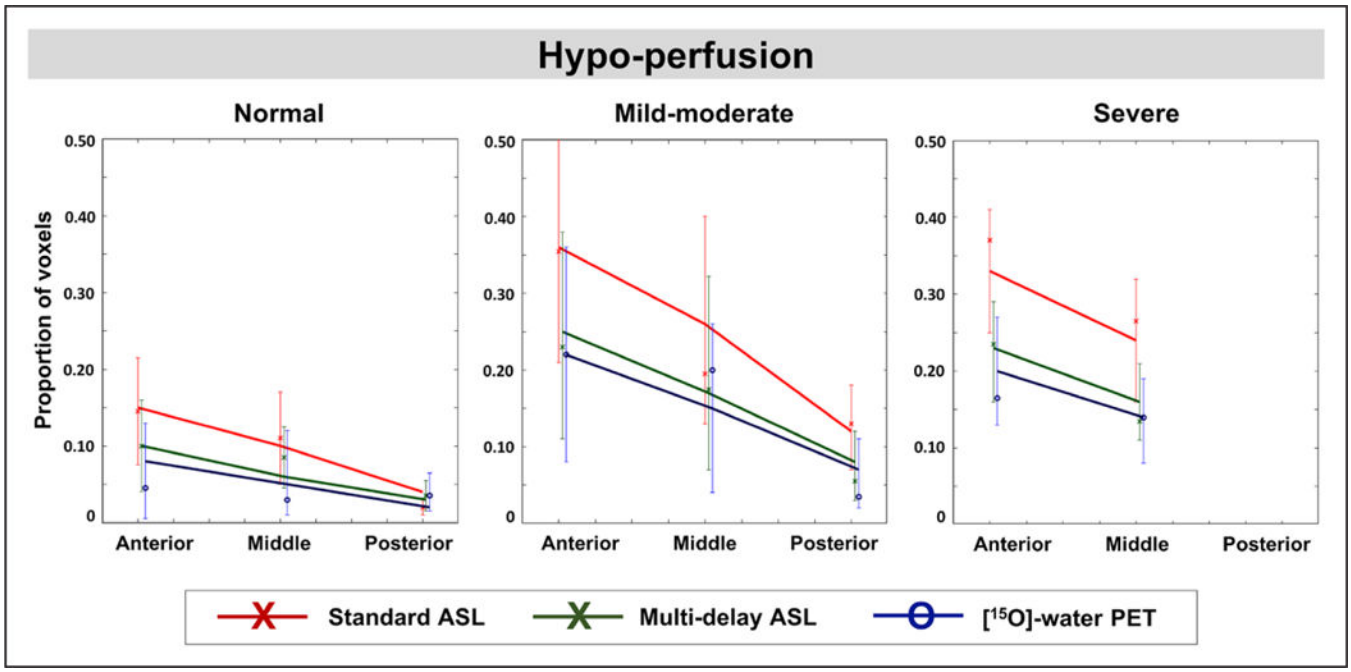

Figure 4.

Regression model predicting the proportion of voxels in each region that is hypoperfused in Moyamoya patients compared with the healthy cerebral blood flow database. Model input factors include region location (anterior, middle, posterior); stenosis severity of the supplying cerebral artery (normal, mildmoderate, severe); and image modality (standard arterial spin labeling [ASL], multidelay ASL, and positron emission tomography [PET]). Solid lines represent regression results, whereas data points represent mean values of measurements and their 95% CIs. None of the posterior cerebral arteries in the Moyamoya group were classified with severe stenosis.

Table 1.

Participant Demographics and Stenosis Characteristics of Moyamoya Patients

Demographics			
	Patients (N=20)	**Healthy Volunteers (N=15)**	
Sex (female, %)	14 (70.0%)	8 (53.3%)	
Age in years (SD, range)	36.8 (9.7, 16–52)	40.9 (12.3, 22–62) *	
Previous stroke (%)	9 (45.0%)	0 (0.0%)	
Patient stenosis characteristics			
Vessel (% for each type)	Normal	Mild-moderate	Severe
Anterior cerebral artery	12 (30.0%)	17 (42.5%)	11 (27.5%)
Middle cerebral artery	6 (15.0%)	12 (30.0%)	22 (55.0%)
Posterior cerebral artery	30 (75.0%)	10 (25.0%)	0 (0.0%) †

* Not significant, P=0.27.

† Posterior regions had fewer vessels with severe stenosis, P<0.001 by Fisher exact test.

Table 2.

Fractional Logistic Regression for Proportion of Voxels With Hypoperfusion in Moyamoya Patients

Hypoperfusion (Fifth Percentile of Healthy Volunteers)					
	Coefficient	**SE**	**95% CI**	**Odds Ratio**	***P* Value**
Method (vs PET)					
Standard ASL	0.68	0.19	(0.31 to 1.05)	1.97	0.003 *
Multidelay ASL	0.16	0.20	(−0.24 to 0.55)	1.17	0.454
Location (vs anterior)					
Middle	−0.44	0.17	(−0.76 to −0.11)	0.64	0.037 *
Posterior	−1.36	0.20	(−1.75 to −0.98)	0.26	<0.001 *
Stenosis (vs normal)					
Mild-moderate	1.14	0.18	(0.78 to 1.50)	3.08	<0.001 *
Severe	1.02	0.19	(0.65 to 1.39)	2.80	0.001 *
Constant	−2.41	0.21	(−2.81 to −2.00)	0.10	…

ASL indicates arterial spin labeling; and PET, positron emission tomography.

* Significant difference in regression model.